

Time domain dynamics of the asymmetric magnetization reversal in exchange biased bilayersD. M. Engebretson,¹ W. A. A. Macedo,^{2,*} Ivan K. Schuller,² P. A. Crowell,¹ and C. Leighton³¹*School of Physics and Astronomy, University of Minnesota, Minneapolis, Minnesota 55455, USA*²*Department of Physics, University of California-San Diego, La Jolla, California 92093, USA*³*Department of Chemical Engineering and Materials Science, University of Minnesota, Minneapolis, Minnesota 55455, USA*

(Received 26 October 2004; published 25 May 2005)

We have explored the dynamics of magnetization reversal asymmetry in exchange biased FeF₂/Fe bilayers using subnanosecond time-resolved Kerr magnetometry. The data reveal an increase in the characteristic precession frequency with decreasing temperature, even above the Néel temperature of the antiferromagnet, which we interpret in terms of the previously observed anisotropy enhancement due to antiferromagnetic spin fluctuations. Below the Néel point the magnetization precession is strongly suppressed due to the damping provided by exchange coupling to the antiferromagnetic layer. Dynamic hysteresis loops measured at a fixed delay between the magnetic field pulse and the optical probe pulse reveal distinct reversal asymmetry that is not observed in the corresponding static loops. The asymmetry takes the form of a suppression of the Kerr rotation signal in the part of the hysteresis loop where nucleation of reverse domains is energetically favorable. The formation of reverse domains prevents the magnetization from rotating coherently on nanosecond time scales. The temperature dependence of this dynamic asymmetry is found to be nonmonotonic and appears to be correlated with the coercivity.

DOI: 10.1103/PhysRevB.71.184412

PACS number(s): 75.70.Cn, 75.30.Gw, 75.40.Gb

I. INTRODUCTION

A rich phenomenology accompanies the exchange shift of the hysteresis loops in antiferromagnet (AF)/ferromagnet (FM) bilayers.^{1,2} Almost 50 years of research on the exchange bias problem³ has revealed some fascinating additional phenomena including coercivity enhancements,^{1,2,4-9} high field rotational hysteresis,^{1,2,10} training effects,^{1,2,11} memory effects,^{1,2,12,13} positive exchange bias,^{1,2,14,15} exchange bias in the paramagnetic state,^{16,17} and a measurement technique dependence.^{1,2,18-20} Recently, considerable attention has been paid to the magnetization reversal mechanisms in AF/FM bilayers,²¹⁻³² primarily due to the realization that the reversal modes can be asymmetric, i.e., the mechanisms of magnetization reversal are different on the two sides of the same hysteresis loop. This is an interesting consequence of the existence of an exchange induced anisotropy and has been investigated in numerous systems using methods such as magneto-optical microscopy,²¹ polarized neutron reflectometry (PNR),^{11,22,23} anisotropic magnetoresistance (AMR),^{23,30,31} magnetic viscosity,^{26,32} Lorentz microscopy,²⁴ and decoration techniques.²⁵

Although many systems show some form of reversal asymmetry, the transition metal difluoride AFs have been shown to exhibit a particularly simple form of the effect in which the reversal occurs largely by rotation on the left side of the hysteresis loop (the descending field branch) and by nucleation of reverse domains on the right side (the ascending field branch).^{22,23,30-34} This was understood in terms of the interplay between the fourfold anisotropy in the FM layer due to perpendicular coupling to a twinned AF, and the unidirectional anisotropy.^{22,23} Krivorotov *et al.* were able to understand this phenomenon in greater detail using the anisotropic magnetoresistance to measure the anisotropy of the FM layer.³¹ These measurements reveal threefold terms in the anisotropy, which were demonstrated unequivocally to be

the origin of the symmetry breaking in the magnetization reversal. These ideas were expanded³⁴ to determine the interfacial coupling strength and the density of uncompensated spins, which are responsible for the exchange bias.³⁵⁻³⁸

Despite this interest in the magnetization reversal mechanisms and the general interest in magnetization dynamics,^{39,40} sweep rate dependent coercivity,^{41,42} and thermal stability in exchange biased systems,³⁴ little has been done to investigate the dynamics of these reversal mechanisms. Frequency domain techniques such as Brillouin light scattering⁴³⁻⁴⁵ and ferromagnetic resonance⁴⁶⁻⁴⁸ have focused primarily on investigations of the spin wave damping and ferromagnetic anisotropy, as opposed to direct study of the reversal mechanisms. In the time domain, picosecond (ps) time resolved measurements have been used to probe the response of AF/FM bilayers to ultrashort laser pulses designed to dynamically disturb or temporarily “unpin” the exchange coupling,⁴⁹ but again magnetization reversal modes were not studied specifically. In this paper we describe the results of subnanosecond time-resolved Kerr effect measurements^{50,51} to probe the dynamics of the asymmetric reversal modes in FeF₂/Fe bilayers.

II. EXPERIMENTAL CONSIDERATIONS

Samples were deposited by high vacuum electron beam evaporation using methods described previously.^{4,14,15,22,23} Samples of structure MgO(100)/FeF₂(110)/Fe(poly)/Al were used, with layer thicknesses of 800, 120, and 30 Å, respectively. The heterostructures were characterized by wide-angle x-ray diffraction and grazing incidence reflectivity. The FeF₂ has a twinned “quasiepitaxial” structure,²³ the Fe overlayers are polycrystalline with (110) texture, and the interfacial roughness is ~6 Å. For comparison MgO(100)/ZnF₂(110)/Fe(poly)/Al samples were also grown (with

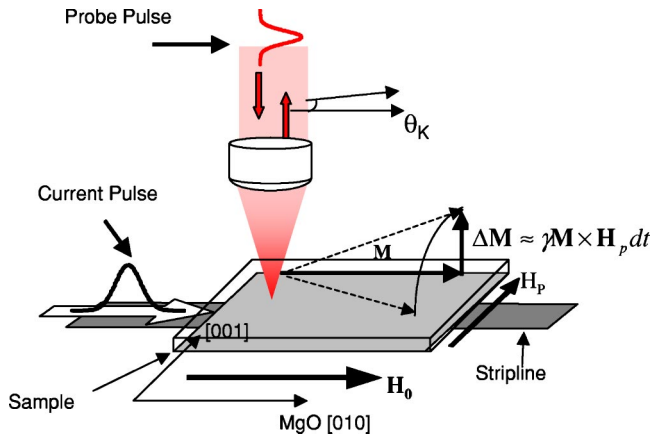


FIG. 1. (Color online). Schematic showing the geometry used in the time resolved Kerr effect experiments. The current pulse injected down the stripline directly underneath the sample induces a field pulse labeled H_p . This induces an out-of-plane magnetization component (the magnetization vector \mathbf{M} and the out-of-plane component due to the tipping pulse $\Delta\mathbf{M}$ are both labeled), which is probed through the Kerr rotation θ_K of the plane of polarization of the probe pulse.

similar layer thickness) to determine which phenomena are due to the exchange coupling between the FM and AF layers (ZnF_2 is not magnetically ordered but is isostructural with FeF_2). The geometry for the time-resolved Kerr magnetometry measurements is shown in Fig. 1. The technique measures the change, ΔM , in the out-of-plane component of the magnetization induced by an ultrafast magnetic field pulse H_p . The temporal width of this pulse is approximately 120 ps at half maximum, and its magnitude is ~ 5 Oe. The pulsed field is applied along the MgO [001] direction and is perpendicular to the applied dc field, which is along the [010] direction. The sample is placed with the ferromagnetic film on top of a tapered microstripline mounted on the cold finger of a helium flow cryostat. To implement the measurement, a 76 MHz train of 150 fs pulses from a mode-locked Ti:sapphire laser operating at a wavelength of 800 nm is split into two beams. One beam is focused on a fast photodiode to generate the magnetic field pulses. The second beam is delayed by a variable time Δt and is focused to a $\sim 25 \mu\text{m}$ diameter spot on the sample. The optical spot is slightly smaller than the width of the stripline. The polar Kerr rotation θ_K of the reflected probe beam is measured using a balanced detector. θ_K is measured as a function of the time delay Δt between the pump and probe pulses, and the results at each time step are averaged over approximately 10^7 laser pulses.

III. RESULTS AND DISCUSSION

Figure 2 shows the temperature dependence of the exchange bias (H_E) and coercivity (H_C) for the FeF_2/Fe (left panel) and ZnF_2/Fe bilayers (right panel) after field cooling in 2 kOe. The data shown are from conventional superconducting quantum interference device (SQUID) magnetometry (solid points) and dynamic hysteresis loops measured by

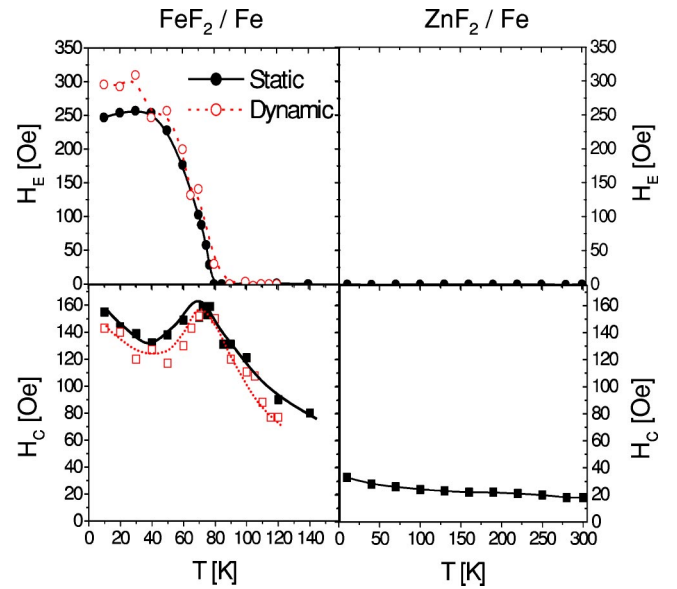


FIG. 2. (Color online). Temperature dependence of the exchange bias (H_E) (top panel) and the coercivity (H_C) (bottom panel) for FeF_2/Fe (AF/FM) (left panel) and ZnF_2/Fe (nonmagnetic/FM) bilayers (right panel). Solid points are from conventional SQUID magnetometry while the open points are from dynamic hysteresis loops as discussed in the text.

the time resolved Kerr effect (open points). The results are similar to that observed in previous work on samples with similar thickness and structure. In FeF_2/Fe H_E displays a monotonic increase with decreasing temperature below T_N as well as a broad peak in H_C near T_N . The ZnF_2/Fe data reveal zero H_E , as expected, and a weak monotonic increase in H_C with decreasing temperature. The peak in $H_C(T)$ near T_N has been observed before in these difluoride systems^{1,52} (as well as other materials),^{53–57} has been studied theoretically,⁹ and is due to the losses that occur in the AF layer when the FM magnetization is reversed as the Néel point is approached. The basic idea is that the losses that occur in the AF part of the AF/FM bilayer increase near T_N . As T_N is approached from below the AF anisotropy decreases rapidly, meaning that reversal of the FM can induce more spin reorientation in the AF layer, and the coercivity increases. This continues until T_N where the AF order is lost and the coercivity begins to decrease again. Hence the broad peak centered around T_N . Various scenarios have been proposed for the exact mechanism for energy loss in the AF. This can be pictured as a consequence of the reduction in anisotropy near T_N in uniform AF layers, leading to an increase in the “dragging” of the AF spins with the FM during reversal.¹ Alternatively, the energy losses could arise from reorientation of “loose” or weakly pinned AF spins at grain boundaries, point defects, or twin boundaries. Finally, it has been proposed⁹ that irreversible energy losses take place in the AF layer and that these are responsible for the peak in $H_C(T)$.

Time resolved measurements on the ZnF_2/Fe “control” layers are discussed first in order to provide an example of the behavior typical of a thin Fe layer, with no exchange coupling present. The data of Fig. 3 show the time evolution of the Kerr rotation from 295 K down to 10 K, for ZnF_2/Fe

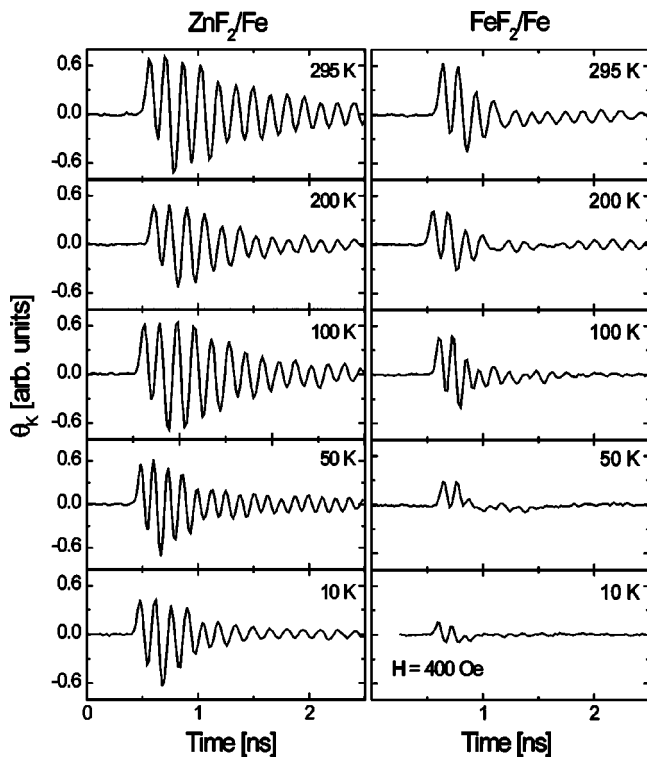


FIG. 3. Time dependence of the Kerr rotation, θ_K , for ZnF_2/Fe (left panel) and FeF_2/Fe (right panel). The data were taken from 295 K (top) to 10 K (bottom). The applied dc magnetic field is 400 Oe.

bilayers (left panel) and FeF_2/Fe bilayers (right panel). Starting with the 295 K ZnF_2/Fe data we observe a clear coherent precession of the magnetization vector in response to the tipping pulse. Note that the (in-plane) tipping pulse is oriented perpendicular to the applied dc field of 400 Oe. The resulting torque tips the magnetization vector out of plane and the Kerr signal observed is sensitive only to this out of plane component. These data therefore only probe the fraction of the magnetization that coherently rotates out of plane in response to the pump pulse. The ZnF_2/Fe precession frequency has a weak temperature dependence, as illustrated in Fig. 4. This frequency is obtained via Fourier transformation of the raw Kerr rotation data, and is directly related to the applied dc field and the anisotropy of the FM layer. Specifically, the precession frequency is given by⁵⁸

$$\omega = |\gamma| \sqrt{\{H_0 + g(\phi)4\pi M_S\} \{H_0 + [1 + f(\phi)]4\pi M_S\}}, \quad (1)$$

where γ is the gyromagnetic ratio, H_0 is the external dc field (in-plane), M_S is the saturation magnetization, and $g(\phi)$ and $f(\phi)$ are functions of the azimuthal angle ϕ of the magnetic field relative to the crystal axes. For an isotropic thin film, $g(\phi) = f(\phi) = 0$, but they will be nonzero in the presence of magnetocrystalline or exchange-induced anisotropies. In the cases considered here, $f(\phi) \ll 1$.⁵⁹ For constant H_0 , as in this case, the data of Fig. 4 on ZnF_2/Fe imply a temperature-independent anisotropy, consistent with the weak temperature dependence of the coercivity (right panel, Fig. 2).

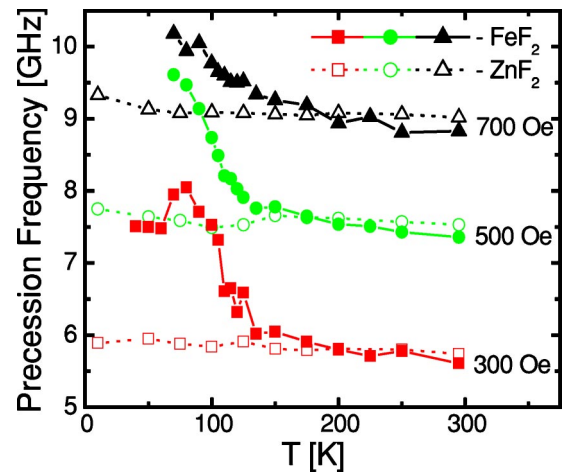


FIG. 4. (Color online). Temperature dependence of the characteristic precession frequency for FeF_2/Fe (solid points) and ZnF_2/Fe (open points) for applied dc magnetic fields of 300, 500, and 700 Oe. These data are extracted from curves of the type shown in Fig. 3 after Fourier transformation of the raw time dependence data.

The right panel of Fig. 3 shows that the situation is different for FeF_2/Fe . A similar behavior is observed at 295 K, well above T_N , but as the temperature decreases the precession frequency shows a marked increase, even above T_N (see Fig. 4). The simplest interpretation of these data is that, even at $T > T_N$, the anisotropy of the FM layer increases with decreasing temperature. Such an effect has been observed before in FeF_2/Fe , both in the temperature dependence of the coercivity and the anisotropy determined from ferromagnetic resonance (FMR), where it was interpreted as an enhancement of the FM anisotropy due to AF spin fluctuations.⁴⁷ Additionally, the time resolved Kerr response of Fig. 3 shows a dramatic suppression of the precession signal below T_N , where the AF order sets in and the FM layer exchange couples to the AF.⁴⁸ The amplitude of the precession signal decreases by a factor of 3 on cooling from 100 to 10 K and at the lowest temperatures no precession can be observed beyond 500 ps. This is consistent with previous measurements of the FMR linewidth^{47,48} and current understanding of the coercivity enhancement in AF/FM bilayers.⁹ The precession signal is decreased by the additional damping provided by the exchange coupling to the AF spins.⁴⁸ The mechanisms by which this occurs will be discussed in more detail below. It is also possible that inhomogeneous dephasing contributes to the suppression of the precession signal.⁶⁰ In either case the additional damping is absent in ZnF_2/Fe bilayers (see Fig. 3), which show no significant change in the precession signal as a function of temperature. In this case the precession can be described by a Gilbert damping parameter, $\alpha = 0.013 \pm 0.002$, which is temperature independent.

As mentioned in Sec. I the motivation for our work is to use the time resolved Kerr technique to probe the dynamics of the magnetization reversal mechanisms, which are known to be asymmetric in these systems. One simple way to probe the field dependence is to acquire isothermal “dynamic hysteresis loops” by measuring the field dependence of the Kerr rotation at a fixed delay between the tipping pulse and the

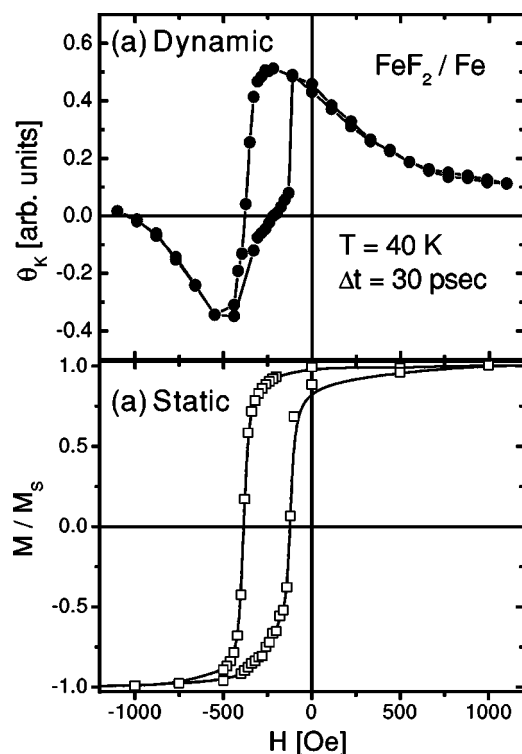


FIG. 5. (a) Dynamic hysteresis loop for FeF_2/Fe at $T=40$ K. These data were taken at a fixed delay between field and probe pulses of 30 ps. (b) Static hysteresis loop (from SQUID magnetometry) at $T=40$ K.

optical probe pulse, as shown in Fig. 5(a) at $T=40$ K. These data were taken at a small delay of 30 ps, which corresponds to the first peak in the precession signal. As noted in Fig. 1, the change ΔM in the magnetization during the pulse is approximately equal to the integral of the torque during the probe pulse. In small fields, the measured Kerr signal should therefore be proportional to the magnetization averaged over the optical spot size, provided that the magnetization can rotate coherently during the pulse. At large magnetic fields, significant precession occurs during the pulse and the Kerr rotation measured at very short delays decreases. When the precession frequency exceeds the bandwidth of the pulse at very large fields, the dynamic magnetization approaches zero. The net result of these effects is a signal with the appearance of a conventional hysteresis loop superimposed on a decaying background at higher fields. It must be emphasized that the hysteresis loops measured in this manner are only sensitive to the part of the magnetization that is able to undergo coherent rotation on subnanosecond time scales, an essential difference to conventional “static” hysteresis loops.

The dynamic loops give H_E and H_C values very similar to those measured by conventional (static) magnetometry, as shown by the agreement between open and solid points in Fig. 2. It is likely that the small deviations are due to the use of different cooling fields for the two data sets (1.1 kOe for dynamic and 2 kOe for static), or unavoidable differences in magnetic field alignment in the two experiments. The unusual phenomenon revealed by the data of Fig. 5(a), which is not observed in the corresponding static loops [Fig. 5(b)], is

the existence of a distinct asymmetric appearance to the dynamic hysteresis loops. [Note that our prior work has shown that the static hysteresis loops appear symmetric despite the strong asymmetries revealed by more direct probes such as PNR²² and AMR.]^{23,30,31,33} The asymmetry observed in the dynamic loops below T_N is observed on the ascending branch of the loop (the right side), and at negative magnetization. This is the point at which the prior investigations of the static reversal asymmetry^{22,23,30-33} have shown that the angular dependence of the anisotropy energy constrains the system to nucleate reverse domains. It can be seen from Fig. 5(a) that the asymmetry manifests itself as a suppression of the Kerr rotation, indicating a reduction in the coherent response to the tipping pulse. This is a direct consequence of the known static reversal asymmetry, which dictates that at this point on the hysteresis loop the favored reversal mode is the nucleation of reverse domains, which would not contribute at all to the Kerr rotation signal. Therefore, due to reverse domain formation the magnetization is unable to respond by coherent rotation on the subnanosecond time scale. The Kerr rotation is close to zero at an applied dc field of $-H_E$, indicating that at this point the coherent precession is completely suppressed. This is consistent with previous PNR measurements²² detecting no coherent rotation on the right side of the hysteresis loop for FeF_2/Fe .

Similar dynamic loop measurements performed between 120 K (above T_N) and 10 K (Fig. 6) reveal an unexpected temperature dependence of the asymmetry. As expected, the asymmetry disappears above T_N , but the temperature dependence is nonmonotonic below this. The maximum asymmetry occurs at 40 K and becomes noticeably weaker at 10 K. This is shown more clearly in Fig. 7 which plots the temperature dependence of the dynamic asymmetry parameter Γ . This quantity is defined by $\Gamma = [1 - (\theta_{\text{ascend}} / \theta_{\text{descend}})]$, where $\theta_{\text{ascend,descend}}$ are the Kerr rotations at $H = -H_E$ on the ascending and descending branches of the hysteresis loops, respectively. The asymmetry parameter is therefore 0 for a completely symmetric loop and 1.0 in the extreme case where the Kerr rotation becomes exactly zero at $H = -H_E$ on the ascending branch (right side) of the dynamic loop. Figure 7 also reveals an intriguing correlation between Γ and the coercivity. Specifically, the dynamic reversal asymmetry is maximized at the point at which the coercivity reaches a minimum. As previously discussed, the peak in $H_C(T)$ at T_N is thought to be a signature of energy losses in the AF layer due to the reversal of the FM layer.¹ This could be due to dragging of “loose” or weakly pinned AF spins when the FM layer reverses, or, as a result of irreversible losses in the AF layer when the FM layer reverses magnetization due to the exchange coupling between the two.⁹ This effect is reduced with decreasing temperature below T_N . At lower temperatures the model of Stiles and McMichael⁹ suggests that the coercivity is then dominated by losses within the FM layer due to inhomogeneities in coupling to the AF. In essence, inhomogeneous local barriers to magnetization reversal exist in the FM layer due to spatial inhomogeneities in the AF/FM coupling strength. This effect leads to the usual increase in coercivity with decreasing temperature. The different temperature dependencies of the two coercive mechanisms therefore result in the existence of a minimum in H_C at some

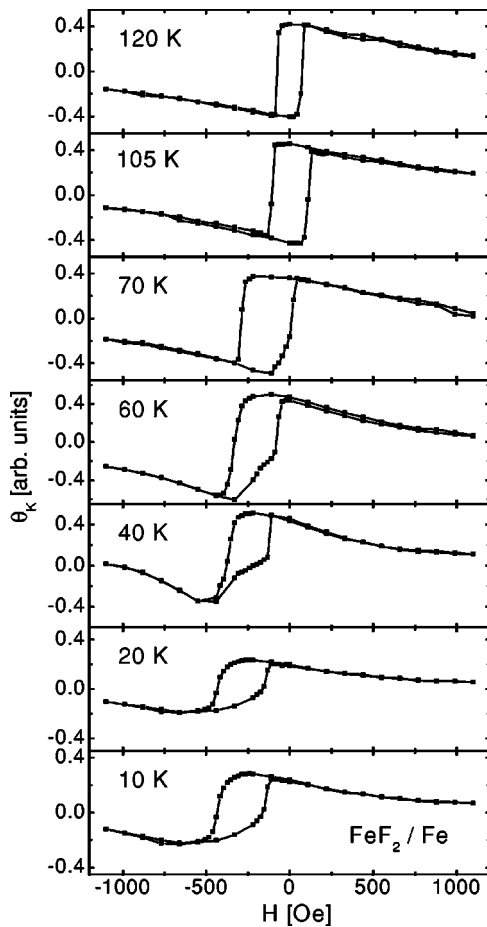


FIG. 6. Temperature dependence of the dynamic hysteresis loops for FeF_2/Fe . These data were taken in a similar manner to those shown in Fig. 5.

intermediate temperature. It is at this point that the dynamic reversal asymmetry is maximized. Although the nonmonotonic temperature dependence of the dynamic asymmetry is not entirely understood it is clear from these data that at $T < 40$ K, where the coercivity begins to increase again with decreasing temperature, the dynamic asymmetry is reduced. Within the framework of the Stiles and McMichael coercivity model this suggests that at low temperatures, when the losses are confined to the FM layer and do not occur in the AF, the asymmetry is decreased. It is possible that in this regime, when the static field is increased beyond the point where reverse domain nucleation occurs on the ascending field branch, the magnetization within the individual domains can respond coherently to the field pulse, restoring the symmetry in the dynamic loops.

We have also carried out time resolved Kerr measurements on MnF_2/Fe , a lower anisotropy counterpart to FeF_2/Fe . This system displays a number of differences including: (i) a weaker damping of the precession signal below T_N ; (ii) smaller dynamic reversal asymmetry; and (iii) a pre-

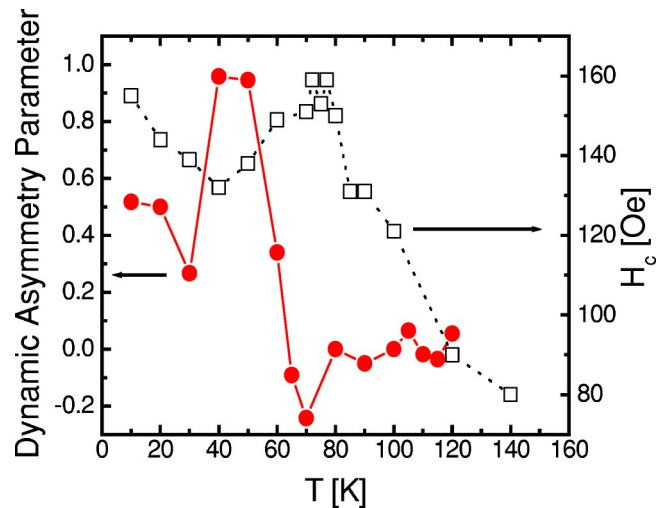


FIG. 7. (Color online). Temperature dependence of the dynamic loop asymmetry parameter, as defined in the text (left axis, solid points). The coercivity extracted from conventional magnetometry measurements is shown for comparison (right axis, open points).

cession frequency which is enhanced only below T_N . The first and second observations are likely due to the smaller exchange induced anisotropy, and therefore exchange bias (by a factor of ~ 4) in MnF_2/Fe compared to FeF_2/Fe . The final observation is consistent with prior FMR data⁴⁶ showing an increase in resonance frequency only below T_N . The absence of FM anisotropy enhancements above T_N is due to the lower susceptibility of the MnF_2 AF, which would reduce the spin fluctuation effects. Note that the coercivity enhancement at $T \gg T_N$ has only been observed in FeF_2/FM systems.^{47,61}

IV. SUMMARY AND CONCLUSIONS

In summary, we have investigated the time domain dynamics of the magnetization reversal asymmetry in FeF_2/Fe . In addition to an increase in FM anisotropy above the Néel temperature of the AF, the data reveal a strong suppression of the magnetization precession below T_N due to the increased damping provided by exchange coupling to the AF layer. Dynamic hysteresis loops show a distinct asymmetry, which does not occur in the corresponding static loops. The asymmetry is due to the suppression of coherent rotation at the magnetic fields where reverse domain nucleation is known to be favorable. This dynamic reversal asymmetry has a non-monotonic temperature dependence which, although it is not entirely understood, displays correlations with the temperature dependence of the coercivity.

ACKNOWLEDGMENTS

Work at UMN was supported by NSF Grant No. DMR 99-83777 and the MRSEC program of the NSF under Grant No. DMR-0212302. Research at UCSD was supported by the US DOE and AFOSR. We would like to thank J. P. Park and M. S. Lund for assistance with data collection.

- *On leave from: Laboratorio de Fisica Aplicado, Centro de Desenvolvimento de Tecnologia Nuclear, 30123-970 Belo Horizonte, Brazil.
- ¹J. Nogués and I. K. Schuller, *J. Magn. Magn. Mater.* **192**, 203 (1999).
 - ²A. E. Berkowitz and K. Takano, *J. Magn. Magn. Mater.* **200**, 552 (1999).
 - ³W. H. Meiklejohn and C. P. Bean, *Phys. Rev.* **102**, 1413 (1956); W. H. Meiklejohn, *J. Appl. Phys.* **33**, 1328 (1962).
 - ⁴C. Leighton, J. Nogués, B. J. Jonsson-Akerman, and I. K. Schuller, *Phys. Rev. Lett.* **84**, 3466 (2000).
 - ⁵S. Zhang, D. V. Dimitrov, G. C. Hadjipanayis, J. W. Cai, and C. L. Chien, *J. Magn. Magn. Mater.* **198–199**, 468 (1999).
 - ⁶Y. J. Tang, B. Roos, T. Mewes, S. O. Demokritov, B. Hillebrands, and Y. J. Wang, *Appl. Phys. Lett.* **75**, 707 (1999).
 - ⁷T. L. Kirk, O. Hellwig, and E. E. Fullerton, *Phys. Rev. B* **65**, 224426 (2002).
 - ⁸Z. Li and S. Zhang, *Phys. Rev. B* **61**, R14897 (2000).
 - ⁹M. D. Stiles and R. D. McMichael, *Phys. Rev. B* **63**, 064405 (2001).
 - ¹⁰M. Takahashi, A. Yanai, S. Taguchi, and T. Suzuki, *Jpn. J. Appl. Phys.* **19**, 1093 (1980).
 - ¹¹U. Welp, S. G. E. te Velthuis, G. P. Felcher, T. Gredig, and E. D. Dahlberg, *J. Appl. Phys.* **93**, 7726 (2003).
 - ¹²N. J. Gokemeijer, J. W. Cai, and C. L. Chien, *Phys. Rev. B* **60**, 3033 (1999).
 - ¹³R. H. Kodama, A. S. Edelstein, P. Lubitz, and S. Sieber, *J. Appl. Phys.* **87**, 5067 (2000).
 - ¹⁴J. Nogués, D. Lederman, T. J. Moran, and I. K. Schuller, *Phys. Rev. Lett.* **76**, 4624 (1996).
 - ¹⁵C. Leighton, J. Nogués, H. Suhl, and I. K. Schuller, *Phys. Rev. B* **60**, 12837 (1999).
 - ¹⁶X. W. Wu and C. L. Chien, *Phys. Rev. Lett.* **81**, 2795 (1998).
 - ¹⁷J. W. Cai, K. Liu, and C. L. Chien, *Phys. Rev. B* **60**, 72 (1999).
 - ¹⁸E. D. Dahlberg, B. Miller, B. Hill, B. J. Jonsson, V. Strom, K. V. Rao, J. Nogués, and I. K. Schuller, *J. Appl. Phys.* **83**, 6893 (1998).
 - ¹⁹J. R. Fermin, M. A. Lucena, A. Azevedo, F. M. de Aguiar, and S. M. Rezende, *J. Appl. Phys.* **87**, 6421 (2000).
 - ²⁰H. Xi, R. M. White, and S. M. Rezende, *Phys. Rev. B* **60**, 14837 (1999).
 - ²¹V. I. Nikitenko, V. S. Gornakov, A. J. Shapiro, R. D. Shull, K. Liu, S. M. Zhou, and C. L. Chien, *Phys. Rev. Lett.* **84**, 765 (2000).
 - ²²M. R. Fitzsimmons, P. Yashar, C. Leighton, I. K. Schuller, J. Nogués, C. Majkrzak, and J. Dura, *Phys. Rev. Lett.* **84**, 3986 (2000).
 - ²³C. Leighton, M. R. Fitzsimmons, P. Yashar, A. Hoffmann, J. Dura, C. F. Majkrzak, and I. K. Schuller, *Phys. Rev. Lett.* **86**, 4394 (2001).
 - ²⁴X. Portier, A. K. Petford-Long, A. de Morais, N. W. Owen, H. Laidler, and K. O'Grady, *J. Appl. Phys.* **87**, 6412 (2000); Y. G. Wang and A. K. Petford-Long, *ibid.* **92**, 6699 (2002); Y. G. Wang, A. K. Petford-Long, T. Hughes, H. Laidler, K. O'Grady, and M. T. Kief, *J. Magn. Magn. Mater.* **242**, 1081 (2002).
 - ²⁵H. D. Chopra, D. X. Yang, P. J. Chen, H. J. Brown, L. J. Swatzen-druher, and W. F. Egelhoff, *Phys. Rev. B* **61**, 15312 (2000).
 - ²⁶I. Panagiotopoulos, N. Moutis, and C. Christides, *Phys. Rev. B* **65**, 132407 (2002).
 - ²⁷O. Hellwig, S. Maat, J. B. Kortright, and E. E. Fullerton, *Phys. Rev. B* **65**, 014418 (2001).
 - ²⁸M. Gierlings, M. J. Prandolini, H. Fritzsche, M. Gruyters, and D. Riegel, *Phys. Rev. B* **65**, 092407 (2002).
 - ²⁹B. Beckmann, U. Nowak, and K. D. Usadel, *Phys. Rev. Lett.* **91**, 187201 (2003).
 - ³⁰C. Leighton, M. Song, and I. K. Schuller, *J. Appl. Phys.* **88**, 344 (2000).
 - ³¹I. N. Krivorotov, C. Leighton, J. Nogués, I. K. Schuller, and E. D. Dahlberg, *Phys. Rev. B* **65**, 100402(R) (2002).
 - ³²C. Leighton and I. K. Schuller, *Phys. Rev. B* **63**, 174419 (2001).
 - ³³A. Inomata, J. S. Jiang, C.-Y. You, J. E. Pearson, and S. D. Bader, *J. Vac. Sci. Technol. A* **18**, 1269 (2000); J. S. Jiang, A. Inomata, C.-Y. You, J. E. Pearson, and S. D. Bader, *J. Appl. Phys.* **89**, 6817 (2001).
 - ³⁴I. N. Krivorotov, C. Leighton, J. Nogués, I. K. Schuller, and E. D. Dahlberg, *Phys. Rev. B* **68**, 054430 (2003).
 - ³⁵K. Takano, R. H. Kodama, A. E. Berkowitz, W. Cao, and G. Thomas, *Phys. Rev. Lett.* **79**, 1130 (1997).
 - ³⁶A. Scholl, F. Nolting, J. Stohr, T. Regan, J. Luning, J. W. Seo, J. P. Locquet, J. Fompeyrine, S. Anders, H. Ohldag, and H. A. Padmore, *J. Appl. Phys.* **89**, 7266 (2001).
 - ³⁷A. Hoffmann, J. W. Seo, M. R. Fitzsimmons, H. Siegwart, J. Fompeyrine, J.-P. Locquet, J. A. Dura, and C. F. Majkrzak, *Phys. Rev. B* **66**, 220406(R) (2002).
 - ³⁸H. Ohldag, A. Scholl, F. Nolting, E. Arenholz, S. Maat, A. T. Young, M. Carey, and J. Stohr, *Phys. Rev. Lett.* **91**, 017203 (2003).
 - ³⁹R. E. Camley, B. V. McGrath, R. J. Astalos, R. L. Stamps, J.-V. Kim, and L. Wee, *J. Vac. Sci. Technol. A* **17**, 1335 (1999).
 - ⁴⁰J. Nogués, J. Sort, S. Surinach, J. S. Munoz, M. D. Baro, J. F. Bobo, U. Luders, E. Haanappel, M. R. Fitzsimmons, A. Hoffmann, and J. W. Cai, *Appl. Phys. Lett.* **82**, 3044 (2003).
 - ⁴¹H. Xi, R. M. White, A. Mao, Z. Gao, Z. Yang, and E. Murdock, *Phys. Rev. B* **64**, 184416 (2001).
 - ⁴²J. Camarero, Y. Pennec, J. Vogel, M. Bonfim, S. Pizzini, M. Cartier, F. Ernult, F. Fetta, and B. Dieny, *Phys. Rev. B* **64**, 172402 (2001).
 - ⁴³P. Miltenyi, M. Gruyters, G. Guntherodt, J. Nogués, and I. K. Schuller, *Phys. Rev. B* **59**, 3333 (1999).
 - ⁴⁴S. M. Rezende, A. Azevedo, M. A. Lucena, and F. M. de Aguiar, *Phys. Rev. B* **63**, 214418 (2001).
 - ⁴⁵A. Ercole, W. S. Lew, G. Lauhoff, E. T. M. Kernohan, J. Lee, and J. A. C. Bland, *Phys. Rev. B* **62**, 6429 (2000).
 - ⁴⁶M. J. Pechan, D. Bennett, N. Teng, C. Leighton, J. Nogués, and I. K. Schuller, *Phys. Rev. B* **65**, 064410 (2002).
 - ⁴⁷C. Leighton, H. Suhl, J. Nogués, and I. K. Schuller, *J. Appl. Phys.* **92**, 1483 (2002).
 - ⁴⁸R. L. Compton, M. J. Pechan, S. Maat, and E. E. Fullerton, *Phys. Rev. B* **66**, 054411 (2002).
 - ⁴⁹G. Ju, A. V. Nurmikko, R. F. C. Farrow, R. F. Marks, M. J. Carey, and B. A. Gurney, *Phys. Rev. Lett.* **82**, 3705 (1999).
 - ⁵⁰M. R. Freeman, *Phys. Rev. Lett.* **69**, 1691 (1992); M. R. Freeman, W. K. Hiebert, and A. Stankiewicz, *J. Appl. Phys.* **83**, 6217 (1998).
 - ⁵¹D. M. Engebretson, J. Berezovsky, J. P. Park, L. C. Chen, C. J. Palmstrom, and P. A. Crowell, *J. Appl. Phys.* **91**, 8040 (2002).
 - ⁵²C. Leighton, M. R. Fitzsimmons, A. Hoffmann, J. Dura, C. F. Majkrzak, M. S. Lund, and I. K. Schuller, *Phys. Rev. B* **65**, 064403 (2002).

- ⁵³C. Hou, H. Fujiwara, K. Zhang, A. Tanaka, and Y. Shimizu, *Phys. Rev. B* **63**, 024411 (2001).
- ⁵⁴S. Poppe, H. Nembach, A. Mougin, T. Mewes, J. Fassbender, and B. Hillebrands (unpublished).
- ⁵⁵F. B. Hagedorn, *J. Appl. Phys.* **38**, 3641 (1967).
- ⁵⁶S. H. Charap and E. Fulcomer, *J. Appl. Phys.* **42**, 1426 (1971).
- ⁵⁷P. A. A. van der Heijden, T. F. M. M. Mass, W. J. M. de Jonge, J. C. S. Kools, F. Roozeboom, and P. J. van der Zaag, *Appl. Phys. Lett.* **72**, 492 (1998).
- ⁵⁸A. H. Morrish, *The Physical Principles of Magnetism* (Wiley, New York, 1965), p. 545.
- ⁵⁹ $f(\phi) \ll 1$ in the limit where all anisotropy fields are small relative to $4\pi M_S$, where M_S is the saturation magnetization. See Ref. 58 for details.
- ⁶⁰Lateral inhomogeneities in the FM layer (on a length scale smaller than the optical spot size) could also result in reduced precession through inhomogeneous dephasing. Although the current measurements are unable to distinguish between these two mechanisms, note that inhomogeneous dephasing would require significant inhomogeneities in either the intrinsic magnetic properties of the FM layer, or the exchange coupling to the AF.
- ⁶¹M. Grimsditch, A. Hoffmann, P. Vavassori, H. Shi, and D. Lederman, *Phys. Rev. Lett.* **90**, 257201 (2003).